

Reduction in frataxin causes progressive accumulation of mitochondrial damage

Gopalakrishnan Karthikeyan¹, Janine H. Santos¹, Maria A. Graziewicz¹,
William C. Copeland¹, Grazia Isaya², Bennett Van Houten¹ and Michael A. Resnick^{1,*}

¹Laboratory of Molecular Genetics, National Institute of Environmental Health Sciences, NIH, Research Triangle Park, NC 27709, USA and ²Departments of Pediatric and Adolescent Medicine and Biochemistry and Molecular Biology, Mayo Clinic and Foundation, Rochester, MN 55905, USA

Received August 6, 2003; Revised and Accepted October 9, 2003

Frataxin protein controls iron availability in mitochondria and reduced levels lead to the human disease, Friedreich's ataxia (FRDA). The molecular aspects of disease progression are not well understood. We developed a highly regulatable promoter system for expressing frataxin in yeast to address the consequences of chronically reduced amounts of this protein. Shutting off the promoter resulted in changes normally associated with loss of frataxin including iron accumulation within the mitochondria and the induction of mitochondrial *petite* mutants. While there was considerable oxidative damage to mitochondrial proteins, the *petites* were likely due to accumulation of mitochondrial DNA lesions and subsequent DNA loss. Chronically reduced frataxin levels resulted in similar response patterns. Furthermore, nuclear DNA damage was detected in a *rad52* mutant, deficient in double-strand break repair. We conclude that reduced frataxin levels, which is more representative of the disease state, results in considerable oxidative damage in both mitochondrial and nuclear DNA.

INTRODUCTION

In organisms capable of aerobic growth, mitochondria play an important role in energy production (ATP synthesis). A by-product of this oxidative phosphorylation process is the formation of reactive oxygen species (ROS). ROS can damage DNA, RNA, proteins and lipids within the cell and they have been implicated in many degenerative diseases, cancer and aging (1,2). There are various defense mechanisms within the mitochondria including anti-oxidant molecules, enzymes that detoxify ROS and repair systems that limit the ROS-mediated damage. When these defenses are overwhelmed, disease may ensue.

Friedreich's ataxia (FRDA) is a progressive neurodegenerative disease with early onset. It results from a deficiency in frataxin, a protein localized to the mitochondria (mt). In typical FRDA patients the gene has undergone a triplet (GAA) expansion within the first intron. This triplet motif can adopt a triple helical DNA structure that inhibits transcription (3,4). The severity of the disease correlates directly with the number of triplet units and consequent decrease in protein levels, with patients having frataxin levels ranging from 6 to 30% of

normal (5). The primary tissues affected in the disease include the large sensory neurons in the dorsal root ganglia and the nucleus dentatus, as well as cardiac and pancreatic cells. The progressive gait and limb ataxia, hypertrophic cardiomyopathy and diabetes mellitus found in FRDA patients are attributed to lowered levels of ATP produced in these energy intensive tissues (6).

Several model systems have been developed in an effort to understand the disease (7,8). In mouse models, deletion of the frataxin gene results in embryonic lethality (8) while its selective inactivation in neuronal and cardiac tissues leads to neurological symptoms and cardiomyopathy associated with mitochondrial iron-sulfur cluster-containing enzyme deficiencies and time-dependent mitochondrial iron accumulation. In contrast, a model expressing 25–35% of wild type frataxin levels by virtue of a (GAA)₂₃₀ expansion inserted in the first intron of the mouse gene has no obvious phenotype (7). Studies using the budding yeast *Saccharomyces cerevisiae* have provided a further understanding of the consequences of frataxin loss (9–13). Deletion of the yeast frataxin homolog *YFH1* results in a 10-fold increase in iron within the mitochondria along with increased ROS production (10,11).

*To whom correspondence should be addressed at: National Institute of Environmental Health Sciences (NIEHS), Mail Drop D3-01, 111 Alexander Drive, Research Triangle Park, NC 27709, USA. Tel: +1 9195414480; Fax: +1 9195417593; Email: resnick@niehs.nih.gov

This leads to loss of mitochondrial function and the appearance of a *petite* phenotype in nearly all strains that have been examined (11,14–16) (see Discussion). In addition, there is the appearance of nuclear DNA damage (9,17,18). Recent studies have shown that frataxin acts as a chaperone for Fe(II) and a storage compartment for excess iron, (17,19–29). This is consistent with the roles played by frataxin in iron export, Fe-S cluster assembly, heme biosynthesis and prevention of oxidative stress.

In recapitulating FRDA in model systems, it is important to be able to examine the consequences of reduced activity and/or progressive changes as the protein level is modified. A system to down-regulate the levels of the protein would be useful in 'humanizing' yeast (30) and making it a more representative model system for the disease. Down-regulation of frataxin has been examined with at least two regulatable on-off promoter systems: *GAL* and *MET25* promoters (15,27). However, the opportunities for varying the levels of expression, at least for *GAL1* regulation (see Results), have not been clear. For example, shutting off the *GAL1* promoter still allows basal expression that for *GAL1-YFH1* is sufficient to complement a frataxin deficiency (see Results). We therefore developed a tightly regulated system for expressing variable levels of frataxin under conditions where there was no detectable basal level expression. This approach allowed us to systematically address the consequences of chronically reduced levels, as well as acute loss, of frataxin *in vivo* and the chronology of events that could eventually lead to mitochondrial dysfunction. As endpoints, we have focused on iron accumulation, mt protein damage, lesions in mtDNA, loss of mtDNA and the appearance of two types of *petites* (ρ^- and ρ^0). Furthermore, with this system we have addressed the impact of modest reductions in frataxin expression on nuclear damage in a recombinational repair-deficient *rad52* strain.

RESULTS

Development of system for rapid reduction in the levels of frataxin using a compromised promoter

A complete loss of frataxin in nearly all yeast backgrounds results in cells losing mitochondrial function and colonies having a small, *petite* appearance (see Discussion) that are unable to grow on glycerol. We wanted to examine the chronology of events associated with reduced levels of frataxin including assessing various kinds of mitochondrial and nuclear damage. This would be more reflective of the human FRDA condition.

To study reduced expression of the frataxin gene, we had initially placed it under the control of the galactose-inducible *GAL1* promoter. However, when this promoter was shut off, the basal level of frataxin expression was sufficient to prevent loss of mitochondrial respiratory function (i.e. there was little if any *petite* formation) (data not shown). This led us to utilize a compromised *GAL1* promoter referred to as *gal1** that results in reduced induction of gene expression (J. Westmoreland, L.K. Lewis and M.A. Resnick, unpublished data). To construct a *gal1** regulated frataxin strain, a fragment containing the *gal1*-YFH1* and the *TRP1* marker was integrated into the *HIS3*

locus of the strain GK2 that contains the *reg1-501* mutation (so that galactose induction is not repressed by glucose) (Fig. 1A) (31). The endogenous *YFH1* gene was then disrupted by gene replacement with the Kanamycin dominant selectable marker so that cells would only express frataxin from the *gal1** promoter when grown in galactose containing medium. This strain, GK178, was used for further experiments.

We followed the frataxin expression levels from this construct using two different assays, western blot analysis of protein levels and quantitative Real-Time PCR amplification of the *YFH1* transcript. During growth in galactose, cells bearing the *gal1*-YFH1* construct contained over 10-fold less frataxin than wild type cells (Fig. 1B). Nevertheless, cells expressing *gal1*-YFH1* grew as well as wild type cells suggesting that there may be a large excess of frataxin in normal cells. By approximately six generations after switching the cells from galactose to glucose, frataxin was not detectable in up to 250 μ g total mitochondrial protein analyzed (Fig. 1B). Consistent with this, frataxin mRNA levels dropped 15–25-fold after the switch to glucose (data not shown). Thus, the low-expressing *gal1** promoter is highly suppressed under repressing conditions.

We determined the appearance of *petites*, as measured by a loss of *grandes*, when cells with the *gal1*-YFH1* construct grown on complex (YPGalactose) or defined (SCGalactose) media, were transferred to glucose-containing media. The appearance of *petites* was measured by plating cells to YPGlucose or YPGlycerol media (*petites* do not grow in YPGlycerol media) at various times. Cells were maintained in log phase growth conditions prior to plating. As shown in Figure 2, there was a rapid decrease in *grandes* so that over 50% cells were *petite* in 7–8 generations when grown in defined medium and 12–13 generations for growth in complex medium. Since *petite* formation trends in both media were similar, we used these media interchangeably depending on the nature of the experiments.

Reduction in frataxin leads to iron accumulation and protein damage prior to *petite* induction

A *petite* phenotype can be the result of mutations in the nucleus and/or mitochondrial DNA or other changes that interfere with respiratory function. The *petites* that result from frataxin deficiency have been attributed to mitochondrial damage since they are efficiently induced in haploids and are not complemented when $\Delta yfh1$ *petite* strains are mated to other *petite* or $\Delta yfh1$ strains (9,16). The loss of frataxin has been shown to cause increased iron levels in the mitochondria that through Fenton chemistry with hydrogen peroxide could lead to OH radicals and damage to mitochondrial macromolecules (9,10,14). We monitored the iron levels within mitochondria isolated from the GK178 strain at different times after the switch to complex glucose-containing media (i.e. frataxin off) by inductively coupled plasma mass spectrometry (ICP-MS). Within five generations, there was a 6–10-fold increase in iron levels within the mitochondria from cells grown in glucose over that of cells grown in galactose (Fig. 3). Thereafter, iron levels steadily increased to 20–30-fold over galactose grown cells. Interestingly, the increase in mitochondrial iron preceded the appearance of *petites* (Fig. 3), suggesting that the *petites* result from an accumulation of damage, not simply an increased level of iron.

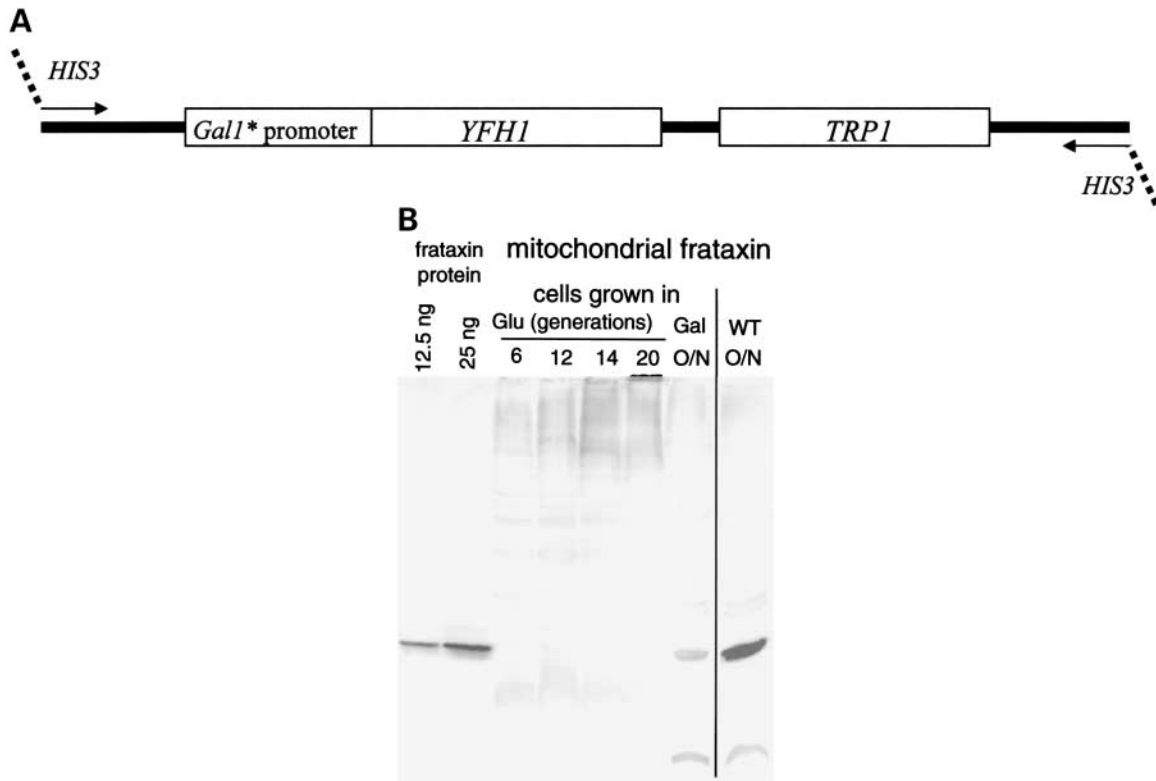


Figure 1. The *gal1** promoter rapidly shuts off frataxin production when cells are transferred to glucose. (A) Schematic of the construct that is integrated into the *HIS3* locus in the strain GK2 that contains the *reg1-501* mutation. (B) Frataxin is not detected by western blot of protein from isolated mitochondria following six generations growth in glucose. Aliquots of 250 μ g of mitochondrial protein was loaded in each lane. Presented are results with *gal1*-YFH1* cells grown galactose (Gal overnight) or transferred to Glucose and grown for up to 19 generations (48 h). Also shown is the frataxin obtained from WT cells (endogenous frataxin promoter) grown overnight in glucose. To estimate protein levels, frataxin standards (12.5 and 25 ng) were included.

The increase in iron levels would be expected to result in the formation of ROS that could lead to mitochondrial protein damage. Oxidized mitochondrial proteins began to appear within two to three generations following the switch to glucose and increased considerably within six to seven generations (Fig. 4). The oxidative lesions were extensive at later times with several species of proteins showing damage. This trend correlates with the progressive increase in mitochondrial iron levels described above. It is likely that such a degree of oxidative damage would have severe consequences for mitochondrial functions, although we have not determined the specific proteins affected.

Petite induction is associated with the appearance of lesions in mtDNA

Changes that could result in *petite* formation include mutations or deletions in the mtDNA as for the case of *rho*⁻ *petites* or complete lack of DNA that is referred to as *rho*⁰. In general, little is known about the appearance of lesions in mtDNA and their impact on the loss of mitochondrial function except for some mtDNA linked human diseases and in a specific yeast strain that allows the measurement of mtDNA damage using an *Arg8* based mutation assay (32,33). Yeast provides the opportunity to address the consequences of lesions in mtDNA since the mitochondrial DNA is dispensable for cell growth.

However, there has been no systematic investigation of ROS derived lesions and how they might lead to the *rho*⁻ or *rho*⁰ categories of mitochondrial mutants. We, therefore, investigated both the appearance of mtDNA damage and the loss of mitochondrial DNA that occur as a consequence of iron mediated ROS.

Damage in mtDNA was determined using a quantitative PCR (QPCR) approach that involves the amplification of a large 6.9 kb DNA fragment (see Materials and Methods) (34–37). During the first round of PCR amplification, the presence of a DNA lesion leads to the inability of the polymerase to synthesize the template DNA because it cannot traverse a lesion. After 18–20 rounds of PCR, the final amount of amplified DNA will be inversely proportional to the number of lesions. Parallel experiments with a 8.5 kb fragment from a different region of the mtDNA gave identical results (data not shown). To estimate the amount of mtDNA present, a small region of the mtDNA is also amplified (~300 bps) since the probability of a lesion appearing within this small target region is comparatively low. Thus, a reduction in large fragment amplification reveals the frequency of DNA lesions while a reduction in the small fragment corresponds to loss of mtDNA. The reduction in large fragment amplification can be attributed directly to number of lesions by normalizing the large fragment amplification to mitochondrial genome copy number (as determined by short fragment amplification) (34,36,38).

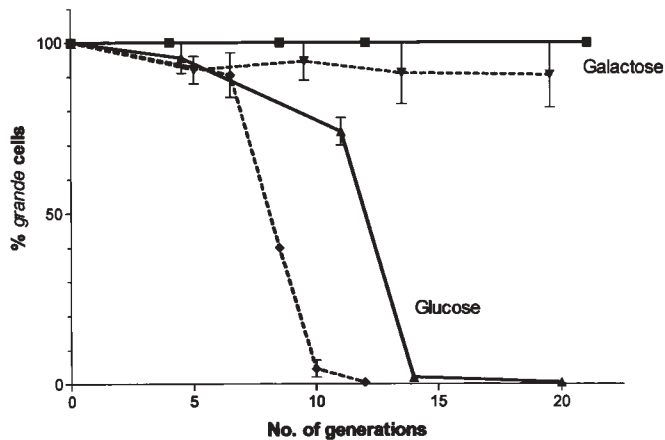


Figure 2. Appearance of *petites* when frataxin is shut off. *gal1*-YFH1* cells that had been grown in galactose were transferred to glucose complex media (solid lines) or defined media (dashed lines) and the logarithmically growing cells were sampled at various times for the ability to give rise to colonies on YPGlycerol plates. Error bars represent SEM.

Lesions in mtDNA were detected about 10 generations after the switch to glucose, corresponding to two to four generations after the increase in iron levels and the appearance of protein oxidative damage (Figs. 5D and 7). *Petites* began to appear soon after, while loss of mtDNA was observed much later (Fig. 5A). By 14 generations, there was almost no mtDNA detectable (Fig. 5A). Under the conditions of acute loss of frataxin, *petites* begin to appear at approximately five lesions per mitochondrial genome (Fig. 5A and D). When 50% of the cells are *petite*, there are approximately 32 lesions per mitochondrial genome. This suggests that oxidative lesions are not complete blocks to *in vivo* replication (see Discussion) and/or they may be subject to repair. It is also possible that there is not a random distribution of lesions among mitochondrial DNA molecules. Regardless of the number of generations in glucose, we were unable to detect damage in a nuclear target using the QPCR assay.

Chronic low levels of frataxin result in a slow accumulation of mtDNA damage

The appearance of mtDNA lesions precedes loss of mtDNA in cells where frataxin levels are greatly reduced and undetectable by western blots. This suggests that under conditions where frataxin levels were reduced there could be an accumulation of lesions and these might lead to alterations in mitochondrial function. Since the *gal1*-YFH1* construct was present in a strain containing a *reg1-501* mutation, the cells could be induced by galactose even in the presence of glucose (which normally represses induction of the *GAL1* promoter). By varying the combination of galactose and glucose, we could modulate the level of frataxin. This was expected to better represent the situation in FRDA patients where frataxin levels are between 5 and 35%. During growth in medium containing 1.5% galactose and 0.5% glucose, ~50% of the cells gave rise to *petites* after about 20 generations. The levels of frataxin transcript were 5–7-fold lower (as compared to 15–25-fold lower in 2% glucose) than those measured during growth in 2% galactose as detected by real-time PCR (data not shown).

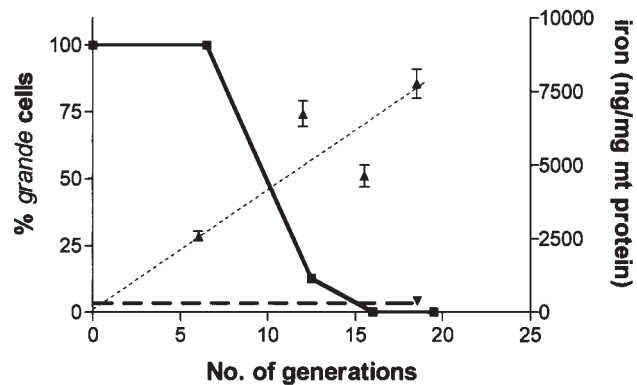


Figure 3. Iron accumulation precedes *petite* formation. Using the growth regime on complex media described in Figure 2, iron levels were examined by ICP-MS analysis. Iron levels are indicated by a small dashed line for growth on glucose and large dashed lines for galactose. Also indicated is the appearance of *petites* (solid line). Error bars represent SEM.

There was a marked difference in the appearance of *petites* between cells experiencing reduced induction of frataxin (Fig. 5B) as compared to no induction (Fig. 5A). The kinetics of lesion accumulation also varied in these different growth conditions. For cells grown in 1.5% galactose + 0.5% glucose, by 16 generations there was a 60% decrease in the amplification of the large 6.9 kb fragment yielding an average of 7.3 lesions per mitochondrial genome. Furthermore, there was only a limited loss of mtDNA from these cells at 22 generations of growth. This suggests a slow accumulation of mtDNA damage. We also observed that mitochondrial lesions can be detected much earlier than *petites*. In contrast, for cells grown in glucose there was complete loss of mtDNA in 16 generations.

The slow rate of accumulation of lesions and eventual loss of mtDNA led us to investigate the nature of the *petites* arising at early and late times using a 'pullback' approach. Cells were grown under conditions of lowered induction of frataxin (1.5% galactose + 0.5% glucose medium) and then plated at five, 11 and 16 generations to medium that would fully induce frataxin expression (2% galactose). A small percentage of colonies that arose at 11 generations were small size. The small colonies were confirmed to be *petites* by their inability to grow on glycerol media while all the large colonies were *grande*. Analysis of mtDNA from *petite* colonies at 11 generations revealed that mtDNA was still present in these cells (but the amount appeared to be reduced) (Fig. 5C). However, *petites* that appeared at the end of 16 generations lacked mtDNA. We did not detect mtDNA even when the number of PCR cycles was increased to 25 suggesting that the *petites* at this stage are *rho*⁰.

We conclude that the *petites* at 11 generations were likely due to point mutations/small deletions within the mtDNA that could impair mitochondrial function. At this time, there was an average of 2.4 lesions per mitochondrial genome. It is interesting that all the *petite* colonies arising from cells plated five generations later did not contain mtDNA. At this time there were approximately 7.3 lesions per mitochondrial genome. This suggests that this level of damage was sufficient to prevent propagation of the mitochondrial genome even after frataxin was fully induced (2% galactose) possibly due to overwhelming the

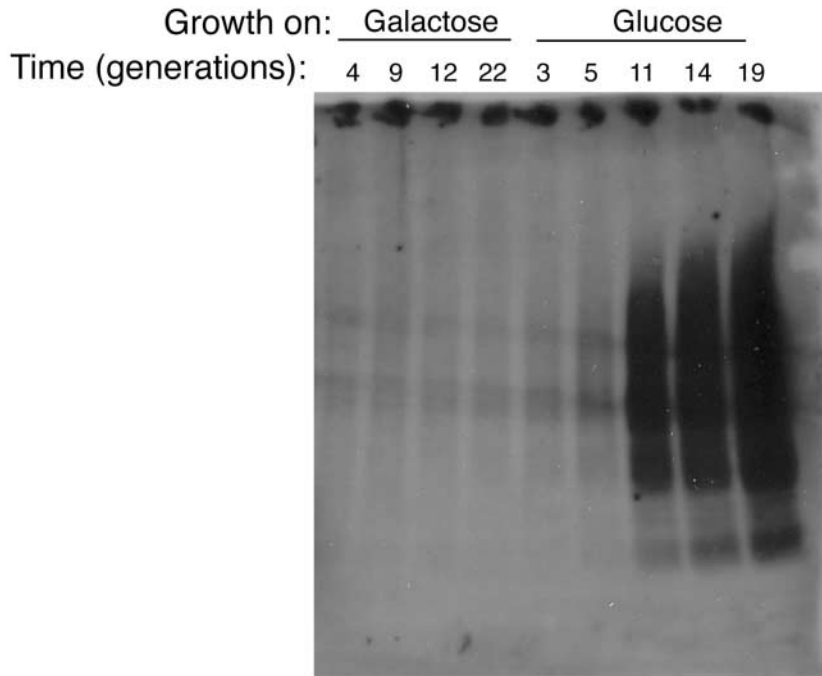


Figure 4. Mitochondrial protein damage increases after a few generations growth in glucose. Using the growth regime on complex media described in Figure 2, protein oxidation was examined by Oxyblot analysis. Presented are results with the *gal1*-YFH1* cells grown on galactose medium for up to 22 generations or transferred to glucose and grown for 19 generations. Growth in galactose results in basal levels of oxidative protein damage (first four lanes). A faint increase in mitochondrial protein damage is observed within two to three generations of growth in glucose and then there is a dramatic increase of oxidized proteins within the mitochondria beginning at 10 h.

DNA repair system and/or blocks to replication. Consistent with this interpretation, there was a sharp decline in amplification of mtDNA (small fragment) when growth was continued in the low induction medium for an additional six generations (i.e. 48 h) (Fig. 5B). It is interesting that we did not find nuclear DNA damage using the QPCR assay in both the growth conditions used. However, the limit of detection of lesions by QPCR is one lesion/ 10^5 bases, thus lower levels of damage would not be detected using this technique.

Nuclear damage response to lowered frataxin levels

Previously, we had demonstrated that in cells lacking frataxin there is an accumulation of nuclear damage, suggesting that frataxin is important for mitochondrial and nuclear genome stability. We have extended those findings with the present system to address nuclear response to reductions in frataxin. Specifically, we wanted to distinguish whether nuclear DNA damage is an early event following frataxin loss or is a later downstream event that arises as a secondary consequence of other physiological changes within the cell.

Since there was limited sensitivity using the QPCR assay to detect low levels of lesions, we used a genetic assay to score nuclear DNA lesions. We examined cell cycle progression following the switch from galactose to glucose medium in the repair proficient GK178 strain and in a strain lacking the *RAD52* gene. Several kinds of DNA damage can lead to the appearance of large budded (dumbbell-shaped) cells due to cell cycle arrest at the G2/M transition (39,40). The *RAD52* gene is required for

the repair of DNA double-strand breaks (DSBs) that can arise in the nucleus.

Shutting off frataxin did not lead to cell cycle arrest in the repair proficient cells (data not shown). These results contrast with those obtained with the *rad52* mutant. Within 3 h after the switch to glucose, there was a small but consistent increase in the G2/M cells and the number of arrested cells increased rapidly to >80% within 9 h (~3–4 generations) (Table 1 and Fig. 6). In addition, we also followed cell cycle progression under conditions of reduced frataxin, when cells were switched to 1.5% galactose and 0.5% glucose. Surprisingly, there was a strong G2/M arrest response even in these growth conditions. To ascertain that this was a nuclear specific response in the sensitized *rad52* strain, we plated cells (at 10 h) to glycerol media and confirmed that they had not become *petite*. This strongly suggests that there is a rapid production of ROS following frataxin loss/reduction that can traverse mitochondrial and nuclear membranes and damage nuclear DNA, possibly leading to DSBs. Interestingly, this was the earliest event that we could detect in our genetic studies, as summarized in Figure 7.

DISCUSSION

Yeast as a model for frataxin deficiency and understanding FRDA

Friedreich ataxia is a mitochondrial-associated disease that occurs due to a reduction in levels of frataxin. Understanding

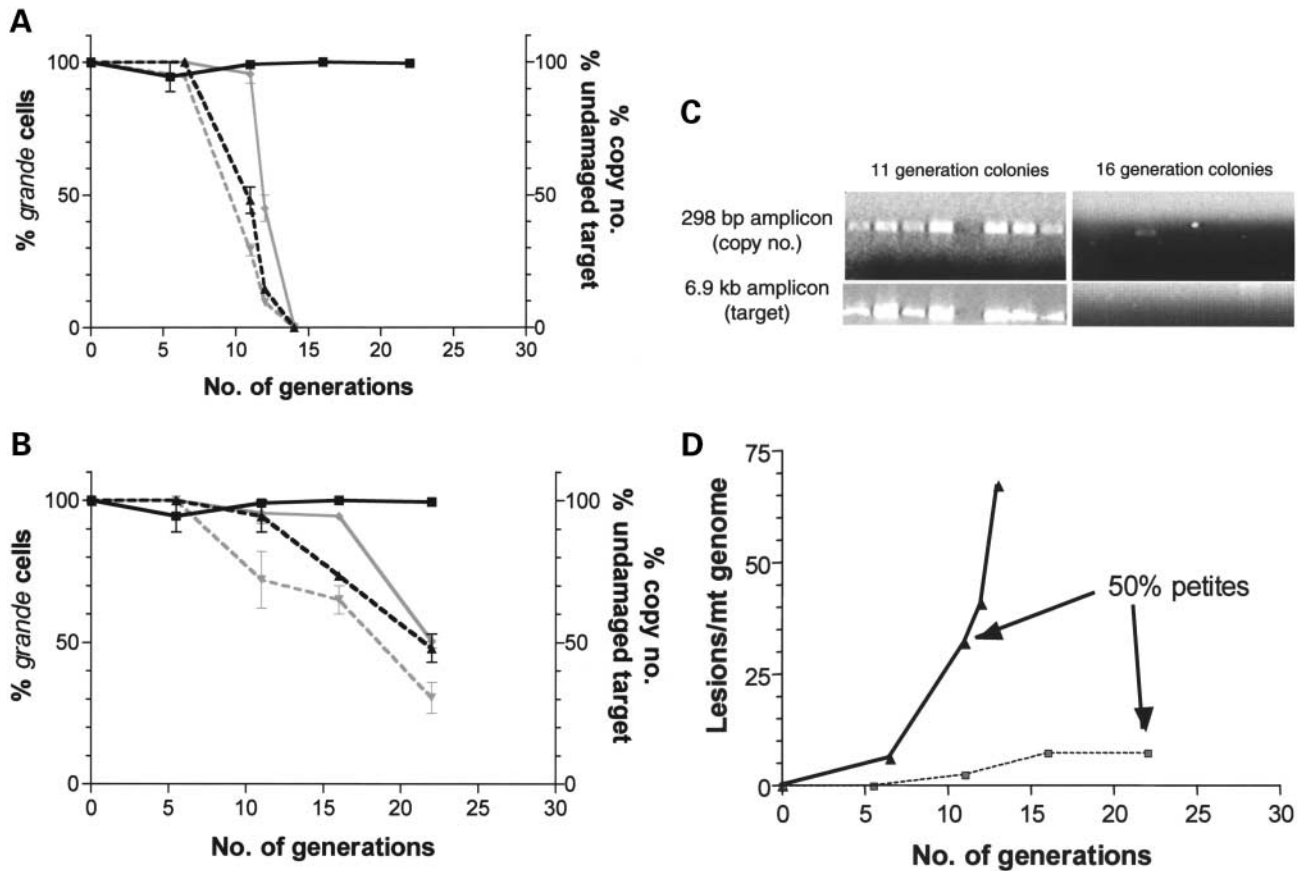


Figure 5. Quantitative PCR reveals extensive mtDNA damage under glucose growth conditions. Using the growth regime on defined media described in Figure 2, mtDNA damage was examined using quantitative PCR analysis. (A) Reduction in copy number (solid gray line) was determined by loss of amplification of a small sequence, while damage was detected as loss of ability to amplify a large target fragment (dashed gray line). The appearance of *petites* is indicated by the dashed black line. Growth on galactose (solid black line) does not generate lesions or *petites*. (B) Following overnight growth in SCGalactose, cells were transferred to 1.5% galactose plus 0.5% glucose. mtDNA damage was examined using quantitative PCR analysis. The symbols are as represented in Figure 5A. (C) Determination of mtDNA in eight *petite* colonies on galactose medium that arose from cells that were first grown in low induction medium for 11 (seven colonies had amplifiable mtDNA) or 16 generations (only one colony had amplifiable mtDNA). (D) Estimated frequency of lesions in mtDNA. Based on the ability to amplify the DNA the number of lesions could be estimated/per mitochondrial genome (see Materials and Methods). Presented are cells grown in glucose (solid black line) or growth in 1.5% galactose and 0.5% glucose (solid gray line). Error bars represent SEM.

Table 1. Cell cycle distribution of $\Delta yfh1 \Delta rad52$ cells transferred to glucose medium (frataxin off) after pregrowth on galactose medium (frataxin on); the percentages are derived from 400 cells

Time in glucose (h)	%G1	%S	%G2
0	30	21	49
3	20	18	62
6	10	12	78
9	8	9	83

the molecular consequences of FRDA can reveal mitochondrial functions and control of ROS, which is also relevant to other human diseases. Since FRDA results from inadequate amounts of protein rather than complete loss, there have been attempts to develop model systems in which the amount of frataxin could be reduced. A mouse 'knock-in' model with a (GAA)₂₃₀ expansion inserted in the first intron of the murine FRDA gene showed no apparent phenotype even though frataxin levels

were reduced to 25–35% of controls (7). The complementation of a frataxin knockout mouse with a transgenic YAC (yeast artificial chromosome) containing the entire human frataxin gene suggests that mice could be developed with YACs derived from FRDA patients containing different lengths of GAA triplets (41). These could provide reduced levels of frataxin, assuming the protein expression is affected similarly to that of humans.

Clearly, model systems in which the level of frataxin can be varied would be useful for understanding the etiology of the disease. The yeast *S. cerevisiae* has been extensively used to address the functions of a variety of human proteins, including those involved in DNA repair (30,42), the human tumor suppressor protein p53 (43,44) as well as frataxin (9,45). Deletion of the frataxin homolog *YFH1* from yeast, results in *petites* in nearly all strains examined, demonstrating an impact on mitochondrial function. Absence of the protein causes an increase in the uptake of iron (12,15). A consequence of the excess iron and the formation of ROS is extensive mitochondrial damage (34). The ROS not only generates *petites*

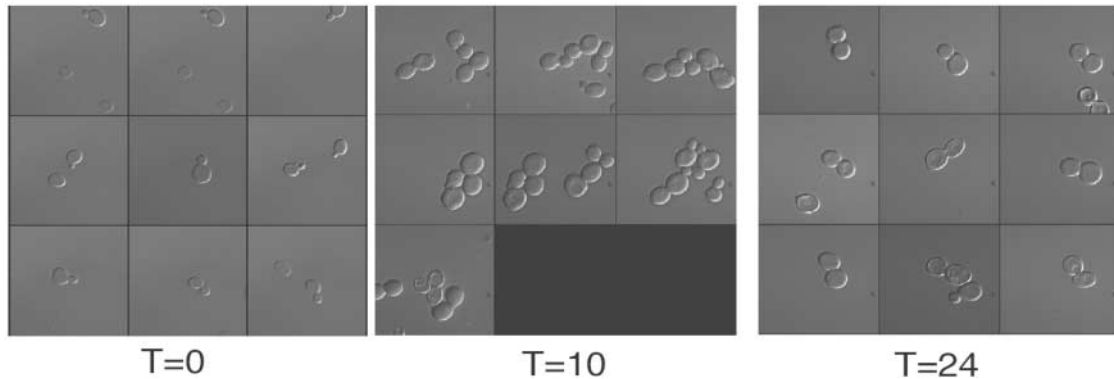


Figure 6. Reduction in the level of frataxin expression leads to rapid cell cycle arrest at G2/M in a *rad52* deletion mutant. Using the growth regime on complex media described in Figure 2, cells were examined microscopically for impact on cell cycle progression. Within 10 h after transfer from YPGalactose to YPGlucose (or within 6 h after transfer from SCGalactose to 1.5% galactose + 0.5% glucose), >80% of the cells are large budded and swollen, typical of yeast cell-cycle arrest at the G2/M stage. Table 1 presents the results for cells in YPGlucose medium.

(10,13,15,16), but frataxin deficiency was recently shown to cause nuclear DNA damage, chromosomal mutations and enhanced recombination rates, presumably via hydrogen peroxide intermediates (9,17,18). These results in yeast correlate with observations with FRDA patients who have exhibited increased levels of 8-hydroxy-2-deoxyguanosine in urine samples (46), increased levels of malondialdehyde, a marker for lipid peroxidation (47) and altered levels of antioxidant enzymes and antioxidants (48,49).

While yeast systems have addressed the consequence of complete loss of frataxin, they have not been used to examine cellular impact of reduced levels of frataxin, which would be more representative of the disease state. Recently, Muhlenhoff *et al.* (27) reported the first use of a galactose regulatable promoter system for shutting off frataxin. However, we suggest that there is a significant basal level when cells are grown on glucose. In the strain background that they used, frataxin may not be completely repressed, since the glucose grown cells are not sensitive to hydrogen peroxide, unlike cells that are completely frataxin deficient (11,27). Furthermore, our attempts to turn off frataxin using a similar *GAL1-YFH1* system were unsuccessful based on only limited *petite* induction when cells were grown on glucose repressing conditions. [We have also found that the wild type *GAL1* promoter has a low basal level of expression under conditions of glucose growth (J. Westmoreland, L.K. Lewis, K.S. Lobachev and M.A. Resnick, unpublished data).]

Thus, to down-regulate frataxin to barely detectable levels, we utilized a mutated version of the galactose promoter *gal1** (J. Westmoreland, L.K. Lewis and M.A. Resnick, unpublished data, sequence available on request). We introduced the *gal1*-YFH1* in a strain with a *reg1-501* mutation which allows induction of the promoter by galactose even in the presence of glucose. This allows a fine-tuning of protein amounts by varying the ratio of glucose and galactose in the growth media. The system enabled us to follow various end-points including *petite* formation, mtDNA and mitochondrial protein damage, iron accumulation and nuclear DNA damage. Moreover, we were able to maintain frataxin at chronic low levels that are expected to better mimic human FRDA conditions.

Consequences of reduction in frataxin levels by *gal1*-YFH1*

Using our *gal1*-YFH1* system, we examined the impact of progressive loss of frataxin. For cells grown on galactose, the level of frataxin was over 10-fold reduced from that with the natural promoter with no discernable phenotype, suggesting a large excess of the protein normally. The excess frataxin found in yeast is probably due to the lack of ferritin in yeast. Biochemical studies have shown that yeast frataxin functions as both a chaperone for Fe(II) and a storage compartment for Fe(III) *in vitro*. These two functions may enable frataxin to promote iron metabolism when iron is limiting, and to prevent iron toxicity when iron is in excess. Thus, a surplus of frataxin within mitochondria could provide a rapid response to sudden increases in iron-sulfur cluster/heme synthesis and/or sudden changes in iron concentration without having to rely upon *de novo* synthesis of frataxin protein.

In our studies we found that within several hours after switching yeast cells from galactose to glucose containing media there were dramatic cellular changes as well as complete loss of frataxin protein. Within six generations no frataxin protein could be detected by western blot (Fig. 1B). Thus, *gal1*-YFH1* provides for tight regulation of the yeast frataxin gene.

A common phenotype for all yeast strains that lack frataxin is that they eventually become *petite*. An exception to this rule was reported for a W303 background strain (11,27). However, when we deleted *YFH1* from this W303 strain by gene replacement with the Kanamycin resistance marker, it became *petite* rapidly. Thus, a simple way to score frataxin deficiency/loss is to monitor *petite* formation. Since *petites* were formed after several generations (Fig. 2A and B), we could follow other changes that preceded *petites* formation and might be representative of events related to reduced levels of frataxin.

Associated with a complete absence of frataxin is the accumulation of iron within the mitochondria. Iron levels increased 6–10-fold within five generations of shutting off frataxin and before the appearance of *petites*, increasing to 20-fold after a few more generations (Fig. 3). It is likely that the

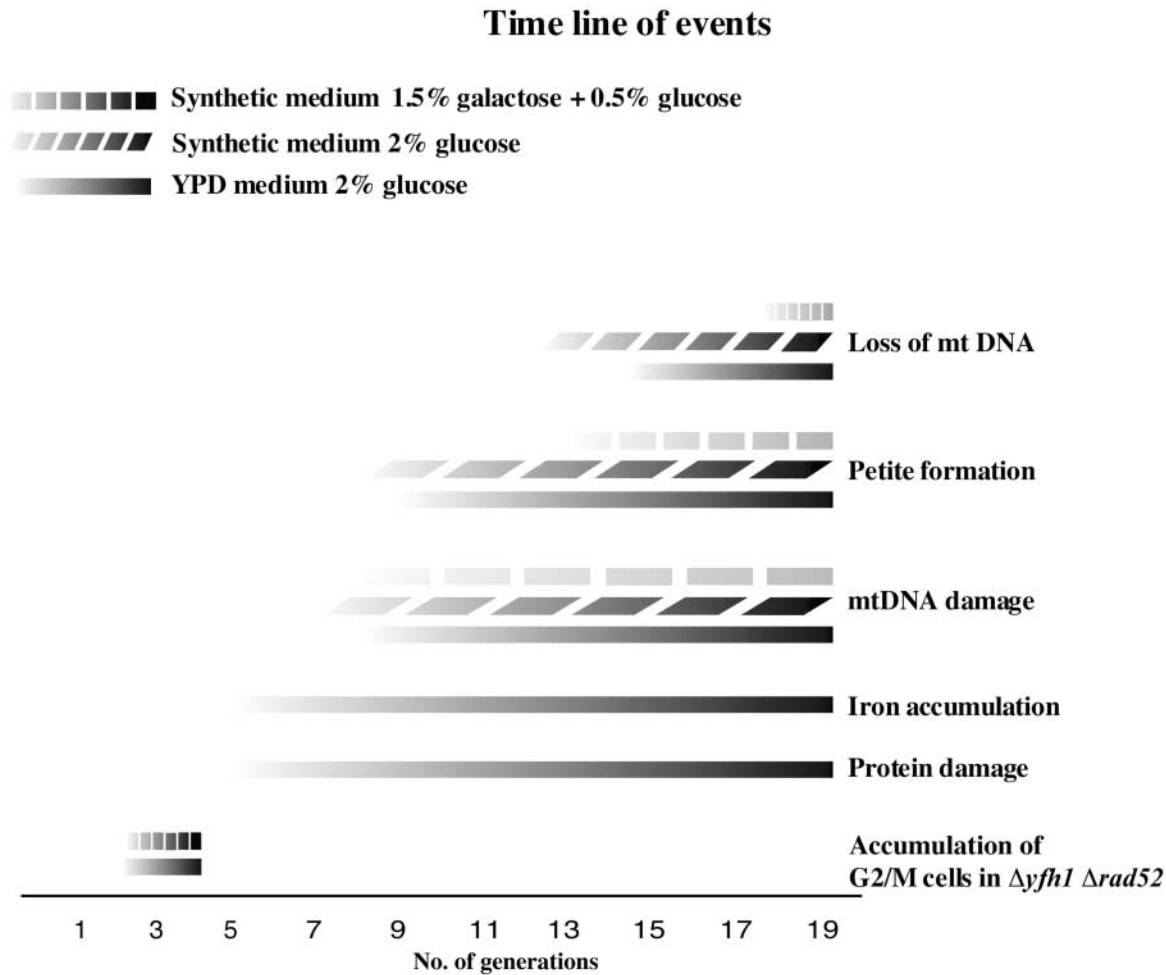


Figure 7. Time line of cellular changes resulting from decreased levels of frataxin. Presented is a summary of changes resulting from growth under conditions of reduced expression levels of frataxin. Complete shut-off: slanted bars (synthetic glucose medium with no galactose) or solid line (complex glucose medium YPD). Chronic low-level expression (synthetic medium containing 1.5% galactose + 0.5% glucose): vertical bars.

early accumulation of iron can lead to the generation of ROS and severe mitochondrial damage. Under conditions of reduced frataxin levels, the appearance of mitochondrial damage is delayed, suggesting a much slower accumulation of iron. This may better reflect observations of mitochondrial iron accumulation in conditional frataxin knockouts in mice. We found that there is an associated appearance of damaged protein that could have many consequences for mitochondrial function in humans and the eventual production of *petites* in yeast. For example, oxidative damage to mitochondrial DNA polymerase could impair its ability to synthesize mtDNA or even perform repair synthesis across lesions generated by ROS. Damage to the respiratory chain components might reduce their efficiency leading to lower ATP production which is one of the hallmark symptoms of FRDA patients (6). Also Fe-S proteins within the mitochondria are very sensitive to oxidative damage. Their loss might lead to alterations in the electron transport pathway, resulting in 'electron leakage' and further accumulation of ROS and damage (2). Thus, mitochondrial protein damage might contribute to the pathology of the disease and might serve as a good biomarker of disease progression in FRDA and is an indicator of increased ROS that also damages lipids and DNA.

The *petite* outcome resulting from loss of frataxin has been attributed to the loss of iron-sulfur cluster biosynthesis (27). However, as determined by the QPCR assay, most *petites* likely arise as a result of the high frequency of DNA lesions and subsequent loss of mtDNA. Even reduced continual expression of frataxin could lead to the accumulation of DNA lesions. While *petites* may not be representative of events associated with mitochondrial defects in humans, they reflect the appearance and consequences of mitochondrial DNA damage. Interestingly, when there were ~32 lesions present per mtDNA copy or one lesion every 2.7 kb of mtDNA, only 50% of the cells were *petite*. There are several explanations for only half of the cells becoming *petite* even though there are a large number of lesions in mtDNA. Possibly there are bypass mechanisms for dealing with mitochondrial lesions in the cell as found in *Xenopus laevis* mtDNA polymerase gamma that can replicate past oxidatively damaged 8-oxo-dG mtDNA lesions (50) as is found for nuclear lesions (51), or there is limited repair. It is even possible that the distribution of lesions is not random. Since there is considerable non-coding DNA in the mitochondrial genome of yeast, lesions within those regions will not have an obvious phenotype. The eventual complete loss of mtDNA

might occur when the repair systems are overwhelmed or when mtDNA polymerase is unable to repair/extend past a lesion.

Even reduced continual expression of frataxin, ~1–3% of wild type, could lead to the accumulation of DNA lesions. However, the results from cells grown on 2% glucose medium differed from those where the level of frataxin was reduced (1.5% galactose + 0.5% glucose). In the latter growth condition, there was a slow accumulation of lesions followed by the appearance of *petites*. This was followed by continued loss of mtDNA (Fig. 5B). This sequence of events suggests that the small number of lesions might yield mutations that cause mitochondrial dysfunction. This is consistent with the observation that the early *petite* colonies retained mitochondrial DNA (Fig. 5C), whereas colonies arising at later times lack mitochondrial DNA. While *petites* in yeast may not be representative of events associated with mitochondrial defects in humans, they reflect the appearance and consequences of mitochondrial DNA damage. The situation of reduced level of frataxin is more consistent with that in FRDA patients and suggests mitochondrial mutations may occur in the mtDNAs of the patients. mtDNA mutations and ROS have been implicated in various cancers (52). Interestingly, gross rearrangements have not been detected in mtDNA from FRDA patients (53). However, sequencing can only reveal small deletions or substitutions. Patients having low levels of frataxin may have some copies of mtDNAs that are mutated so that the mitochondria would be heteroplasmic. The combination of mitochondrial mutations, altered proteins, excess iron and increased ROS could contribute significantly to the disease state.

Not only do reduced levels of frataxin have a broad range of impacts on mitochondria, we found that there was a dramatic cell signaling response that could be detected in the *rad52* mutant. Previously, we demonstrated the nuclear genome of yeast to be at-risk when cells completely lacked frataxin (9). Surprisingly, the earliest detectable event under both conditions of growth (2% glucose and 1.5% galactose + 0.5% glucose) in a *rad52* mutant was the accumulation of large-budded G2/M cells. This suggests the production of ROS even in reduced frataxin expression is sufficient to enter the nucleus and interact with chromosomal DNA. Another possibility might be that a disruption in the mitochondria could signal changes in the nucleus that lead to chromosomal damage, possibly an apoptotic-like response. Since the *RAD52* gene is required for the recombinational repair of double-strand breaks in chromosomal DNA, these results suggest that DSB lesions are produced. They could be induced directly by ROS or could arise during replication of single-strand lesions. Also, Lesuisse *et al.* (17) reported spontaneous reversion to cells capable of growth on glycerol medium in a lawn of *petite* mutants. Possibly, this is due to nuclear DNA damage in cells lacking frataxin. Surprisingly, strong G2/M arrest occurred within 6 h after reducing frataxin expression, much earlier than the induction of *petites*.

These results with the sensitive *rad52* mutant suggest that nuclear DNA damage is an important consequence of reduced frataxin expression. Possibly, the cells of patients with severe FRDA symptoms also experience nuclear DNA damage. Much of this might be repairable, but it still represents a potential threat to genome stability. We suggest that various markers of nuclear DNA damage in mammalian FRDA systems including the activation of p53 be examined. In this context, it is

interesting that frataxin may also provide signals for apoptosis directly or indirectly and play a role in the differentiation of particular cell types (54).

Overall consequences of frataxin deficiency and implications for other mitochondrial diseases

Using our highly regulatable system for the expression of frataxin, we have been able to map the timeline of cellular changes including progressive mitochondrial dysfunction resulting from reduced levels of frataxin. As shown in Figure 7, the pattern of changes is similar for both growth conditions (2% glucose and 1.5% galactose + 0.5% glucose). However, for the latter case of chronic low-level expression of frataxin, which is more representative of the situation in FRDA, the various steps could be more easily resolved. Clearly the first change is a nuclear effect that can only be detected in a repair-deficient mutant. Apparently, the levels of ROS increase subsequently to the point where iron accumulates and protein is damaged. Eventually, this leads to the appearance of mitochondrial DNA lesions, followed later (under conditions of low frataxin expression) by the loss of mitochondrial genomes.

These results with controlled frataxin expression have implications for other diseases. ROS generated within the mitochondria have been implicated in a wide variety of neurodegenerative diseases and aging (2). For example, increased free radical production due to reduced *SOD1/2* activity and complex I defects have been implicated in amyotrophic lateral sclerosis (ALS) and Parkinson's disease pathologies respectively (55). There is also evidence for increased oxidative damage to mtDNA in neurodegenerative disorders such as Alzheimer's and Parkinson's disease due to the high energy demand in synapses which leads to increased stress (56–58). Impaired mitochondrial energy production has also been linked to physiological symptoms in Huntington's disease (59).

The present results are the first to demonstrate that quantitative reduction in a protein that prevents ROS accumulation can lead to progressive changes in mitochondrial and nuclear functions. Chronic low levels of frataxin expression achieved utilizing the *gal1** system causes an increase in ROS production that damages mtDNA. This damage occurs over several generations and, for the case of frataxin reduction, provides a window of opportunity in which to test various therapeutic agents to alleviate this oxidative stress. One of the endpoints, *petite* formation, is easy to score and could be used to screen for chemicals that would ameliorate the consequences of lowered frataxin expression. This approach with reduced frataxin levels could also be employed to identify agents that might generally reduce oxidative damage in mitochondria, which would be valuable in treating other neurodegenerative diseases.

MATERIALS AND METHODS

Yeast strains and general genetic and molecular methods

Growth and strains. Yeast cells were grown at 30°C on standard YP (yeast extract 1%, peptone 2%) or synthetic complete (SC) media (60). The carbon sources were either glucose or

galactose and were at 2% concentration. Yeast transformation and gene disruption were performed according to the methods of Gietz and Schiestl (61). Oligonucleotides for *YFH1* gene disruption, tailed primers to clone the *YFH1* gene into pRSgal1* and to insert the *gal1*-YFH1*, *TRP* cassette into the *HIS3* locus were purchased from Life Technologies (Invitrogen, Carlsbad, CA). The following strain was employed for this study: GK178 (*MATa ade5-1 leu2-3, 112 trp1-289 ura3-52 reg1-501 Ayfh1::G418 his3::gal1*-YFH1*) derived from CG379 (62).

Petite formation assays. GK178 cells were grown on synthetic or complex galactose containing media and transferred to glucose media at 1×10^6 cells/ml. Cells were plated on YPGlucose, YPGalactose or YPGlycerol containing media and incubated for 2 days at 30°C. The data are presented as the percent of colonies formed on YPGlycerol plates compared to the YPGlucose plates.

Nuclear DNA damage assay. Nuclear DNA damage was monitored as an accumulation of G2/M large-budded swollen cells as described (40). Briefly, cells were sampled at various time points and scored for unbudded, small budded and large budded cells under a microscope. The numbers represent an average of 400 cells per time point.

Iron estimation

Cells were grown on YPGalactose medium and inoculated in YPGlucose medium at 1×10^6 cells/ml. The cells were maintained in log phase throughout the experiment by constant re-inoculation in fresh media. At various times cells were harvested, mitochondria isolated (63) and resuspended in metal determination buffer (64) to a final protein concentration of 2.5 mg/ml. Duplicate samples (200 μ l each) were analyzed by inductively coupled plasma mass spectrometry (ICP-MS) (65) at the Mayo Metals Laboratory.

Mitochondrial protein oxidation

Mitochondria preparation. Yeast cells were grown as described for iron estimation. An aliquot of ~ 5 ml wet pellet of cells was resuspended in 2 volumes of mannitol buffer (210 mM mannitol, 70 mM sucrose, 5 mM Tris-HCl pH 7.5, 5 mM EDTA) and distributed in microcentrifuge tubes (1 ml to each tube). About 200 μ l of 425–600 microns acid washed glass beads (SIGMA) were added to the tubes and the cells were vortexed for 5 min three times with 3 min intervals on ice. This step was followed by gentle centrifugation (20g for 5 min) in order to remove glass beads and unbroken cells. The supernatant was centrifuged at 6400g for 20 min. Pellets were resuspended in 5 ml of cold mannitol buffer. Mitochondria were purified from this pellet with a two-step discontinuous sucrose gradient (66); the mitochondrial fraction bands at the interface of the two sucrose solutions. The mitochondria were diluted in 4 volumes of mannitol buffer, polluted and washed two times with the buffer to remove any nuclear DNA or protein that may be stuck to them. They were then lysed by boiling for 30 s in 2% SDS, 10% glycerol, 20 mM Tris-HCl pH 8.0, 0.2 mM EDTA and 14 mM β -mercaptoethanol. The lysates were centrifuged for 2 h at 16 000g (Eppendorf 5415C micro-centrifuge). Protein

concentration in the supernatant was determined using a BCA Protein Assay Reagent Kit (PIERCE, Rockford, IL) and was typically 1.0–1.5 mg/ml. The extracts were concentrated using micro-concentrators (Micron 30) to approximately 10 mg/ml. They were then frozen in liquid nitrogen, stored at -80°C and used to determine the level of yeast mitochondrial protein oxidation.

Detection of protein oxidation. Carbonyl groups are formed at some amino acid residues as a result of protein oxidation. These groups were immunologically detected in proteins using an OxyBlot kit (Intergen NY). An aliquot of 50 μ g of protein extract was treated with 2,4-dinitrophenylhydrazine (DNPH) to derivatize the carbonyl groups to 2,4-dinitrophenylhydrazone (DNP-hydrazone) as previously described for mitochondrial proteins (67). They were then separated on a 4–20% polyacrylamide gel and transferred to an Immobilon-P membrane (Millipore). The membrane was probed with primary antibody specific to the DNP-hydrazone moiety in the proteins and then with horseradish peroxidase conjugated secondary antibody against the primary antibody. Membranes were then treated with ECL Plus Western Blotting Detection Reagents (Amersham Pharmacia, Piscataway, NJ) and detected by autoradiography.

Mitochondrial DNA damage

DNA isolation and DNA damage analysis by QPCR. High molecular weight DNA was extracted using the MasterPure Yeast DNA purification kit from Epicentre (Madison, WI). Nuclear and mtDNA integrity and copy number were analyzed using QPCR assay (37). Genomic DNA is isolated and specific primers are used to amplify a fragment of the mitochondrial and/or nuclear DNA. In the present study, five different fragments were amplified: one in the nucleus and four in the mitochondrial genome. Relative amplification was calculated comparing amplification of glucose grown cells with cells grown on galactose. These values are next used to estimate the average number of lesions per 10 kb of the genome, assuming a Poisson distribution (35,37). The DNA targets analyzed in the present study were as follows: (i) 16.4 kb nuclear region encompassing genes *Rad14*, *PFK2* and *HFA1* on chromosome XIII, using primers 5'-TAG TAG GGC TAA CGA CGG TGA TC-3' (666791) and 5'-CGC TAA AAT CCC GTG TAT CCC TTG-3' (683201); (ii) 6.9 kb mito fragment starting at the 5' flanking region of the COX1 gene amplified with oligonucleotides 5'-GTG CGT ATA TTT CGT TGA TGC GT-3' (13999) and 5'-GTC ACC ACC TCC TGC TAC TTC AA-3' (20948); (iii) 8.5 kb mito segment encompassing the whole subunit 6 of the ATPase gene, using primers 5'-AAT GCA TTT TTT AGG TAT TAA TGG-3' (26377) and 5'-CAA TTT ATA TAT TAA TAG TTC CGG-3' (34919). The short fragments were obtained using (iv) 5'-TGG AGC AGG TAT CTC AAC AA-3' and 5'-TGT AGC TTC TGA TAA GGC GA-3' a 158 bp target inside the ATPase subunit 9 gene and (v) 5'-TTC ACA CTG CCT GTG CTA TCT AA-3', which in combination with the oligonucleotide 13999 gives rise to the 298 bp mito

fragment. Results presented here are the mean of two sets of PCR amplifications for each target gene of at least three different biological experiments.

ACKNOWLEDGEMENTS

We would like to thank Oleksander Gakh for the western blots with mitochondrial proteins for detecting frataxin, Mythreye Karthikeyan for help with the G2-arrested yeast cell pictures and Francoise Foury for the W303 strain. We also thank Homa Azargoon for technical assistance and Kevin Lewis and Jim Westmoreland for the development of the *gal1** promoter and Greg Stuart and Ron Mason for critical reading of the manuscript. G.I. is funded by grant AG15709 from the NIH/NIA.

REFERENCES

- Beal, M.F. (2000) Energetics in the pathogenesis of neurodegenerative diseases. *Trends Neurosci.*, **23**, 298–304.
- Mandavilli, B.S., Santos, J.H. and Van Houten, B. (2002) Mitochondrial DNA repair and aging. *Mutat. Res.*, **509**, 127–151.
- Grabczyk, E. and Usdin, K. (2000) The GAA*TTC triplet repeat expanded in Friedreich's ataxia impedes transcription elongation by T7 RNA polymerase in a length and supercoil dependent manner. *Nucl. Acids Res.*, **28**, 2815–2822.
- Sakamoto, N., Chastain, P.D., Parniewski, P., Ohshima, K., Pandolfo, M., Griffith, J.D. and Wells, R.D. (1999) Sticky DNA: self-association properties of long GAA.TTC repeats in R.R.Y triplex structures from Friedreich's ataxia. *Mol. Cell.*, **3**, 465–475.
- Campuzano, V., Montermini, L., Lutz, Y., Cova, L., Hindelang, C., Jiralerspong, S., Trottier, Y., Kish, S.J., Faucheux, B., Trouillas, P. *et al.* (1997) Frataxin is reduced in Friedreich ataxia patients and is associated with mitochondrial membranes. *Hum. Mol. Genet.*, **6**, 1771–1780.
- Lodi, R., Cooper, J.M., Bradley, J.L., Manners, D., Styles, P., Taylor, D.J. and Schapira, A.H. (1999) Deficit of *in vivo* mitochondrial ATP production in patients with Friedreich ataxia [see comments]. *Proc. Natl Acad. Sci. USA*, **96**, 11492–11495.
- Miranda, C.J., Santos, M.M., Ohshima, K., Smith, J., Li, L., Bunting, M., Cossee, M., Koenig, M., Sequeiros, J., Kaplan, J. *et al.* (2002) Frataxin knockin mouse. *FEBS Lett.*, **512**, 291–297.
- Cossee, M., Puccio, H., Gansmuller, A., Koutnikova, H., Dierich, A., LeMeur, M., Fischbeck, K., Dolle, P. and Koenig, M. (2000) Inactivation of the Friedreich ataxia mouse gene leads to early embryonic lethality without iron accumulation. *Hum. Mol. Genet.*, **9**, 1219–1226.
- Karthikeyan, G., Lewis, L.K. and Resnick, M.A. (2002) The mitochondrial protein frataxin prevents nuclear damage. *Hum. Mol. Genet.*, **11**, 1351–1362.
- Babcock, M., de Silva, D., Oaks, R., Davis-Kaplan, S., Jiralerspong, S., Montermini, L., Pandolfo, M. and Kaplan, J. (1997) Regulation of mitochondrial iron accumulation by Yfh1p, a putative homolog of frataxin. *Science*, **276**, 1709–1712.
- Foury, F. and Cazzalini, O. (1997) Deletion of the yeast homologue of the human gene associated with Friedreich's ataxia elicits iron accumulation in mitochondria. *FEBS Lett.*, **411**, 373–377.
- Foury, F. and Talibi, D. (2000) Mitochondrial control of iron homeostasis. A genome wide analysis of gene expression in a yeast frataxin deficient mutant. *J. Biol. Chem.*, **276**, 7762–7768.
- Koutnikova, H., Campuzano, V., Foury, F., Dolle, P., Cazzalini, O. and Koenig, M. (1997) Studies of human, mouse and yeast homologues indicate a mitochondrial function for frataxin. *Nat. Genet.*, **16**, 345–351.
- Puccio, H. and Koenig, M. (2000) Recent advances in the molecular pathogenesis of Friedreich ataxia. *Hum. Mol. Genet.*, **9**, 887–892.
- Radisky, D.C., Babcock, M.C. and Kaplan, J. (1999) The yeast frataxin homologue mediates mitochondrial iron efflux. Evidence for a mitochondrial iron cycle. *J. Biol. Chem.*, **274**, 4497–4499.
- Wilson, R.B. and Roof, D.M. (1997) Respiratory deficiency due to loss of mitochondrial DNA in yeast lacking the frataxin homologue. *Nat. Genet.*, **16**, 352–357.
- Lesuisse, E., Santos, R., Matzanke, B.F., Knight, S.A., Camadro, J.M. and Dancis, A. (2003) Iron use for haeme synthesis is under control of the yeast frataxin homologue (Yfh1). *Hum. Mol. Genet.*, **12**, 879–889.
- Bidichandani, S.I., Purandare, S.M., Taylor, E.E., Gumin, G., Machkhas, H., Harati, Y., Gibbs, R.A., Ashizawa, T. and Patel, P.I. (1999) Somatic sequence variation at the Friedreich ataxia locus includes complete contraction of the expanded GAA triplet repeat, significant length variation in serially passaged lymphoblasts and enhanced mutagenesis in the flanking sequence. *Hum. Mol. Genet.*, **8**, 2425–2436.
- Adinolfi, S., Trifuoggi, M., Politou, A.S., Martin, S. and Pastore, A. (2002) A structural approach to understanding the iron-binding properties of phylogenetically different frataxins. *Hum. Mol. Genet.*, **11**, 1865–1877.
- Adamec, J., Rusnak, F., Owen, W.G., Naylor, S., Benson, L.M., Gacy, A.M. and Isaya, G. (2000) Iron-dependent self-assembly of recombinant yeast frataxin: implications for Friedreich ataxia. *Am. J. Hum. Genet.*, **67**, 549–562.
- Gakh, O., Adamec, J., Gacy, A.M., Twesten, R.D., Owen, W.G. and Isaya, G. (2002) Physical evidence that yeast frataxin is an iron storage protein. *Biochemistry*, **41**, 6798–6804.
- Cavadini, P., O'Neill, H.A., Benada, O. and Isaya, G. (2002) Assembly and iron-binding properties of human frataxin, the protein deficient in Friedreich ataxia. *Hum. Mol. Genet.*, **11**, 217–227.
- Park, S., Gakh, O., Mooney, S.M. and Isaya, G. (2002) The ferroxidase activity of yeast frataxin. *J. Biol. Chem.*, **277**, 38589–38595.
- Nichol, H., Gakh, O., O'Neill, H.A., Pickering, I.J., Isaya, G. and George, G.N. (2003) Structure of frataxin iron cores: an X-ray absorption spectroscopic study. *Biochemistry*, **42**, 5971–5976.
- Park, S., Gakh, O., O'Neill, H.A., Mangravita, A., Nichol, H., Ferreira, G.C. and Isaya, G. (2003) Yeast frataxin sequentially chaperones and stores iron by coupling protein assembly with iron oxidation. *J. Biol. Chem.*, **5**, 5.
- Yoon, T. and Cowan, J.A. (2003) Iron-sulfur cluster biosynthesis. Characterization of frataxin as an iron donor for assembly of [2Fe-2S] clusters in ISU-type proteins. *J. Am. Chem. Soc.*, **125**, 6078–6084.
- Muhlenhoff, U., Richhardt, N., Ristow, M., Kispal, G. and Lill, R. (2002) The yeast frataxin homolog Yfh1p plays a specific role in the maturation of cellular Fe/S proteins. *Hum. Mol. Genet.*, **11**, 2025–2036.
- Duby, G., Foury, F., Ramazzotti, A., Herrmann, J. and Lutz, T. (2002) A non-essential function for yeast frataxin in iron-sulfur cluster assembly. *Hum. Mol. Genet.*, **11**, 2635–2643.
- Chen, O.S., Hemenway, S. and Kaplan, J. (2002) Inhibition of Fe-S cluster biosynthesis decreases mitochondrial iron export: evidence that Yfh1p affects Fe-S cluster synthesis. *Proc. Natl Acad. Sci. USA*, **99**, 12321–12326.
- Resnick, M.A. and Cox, B.S. (2000) Yeast as an honorary mammal. *Mutat. Res.*, **451**, 1–11.
- Hovland, P., Flick, J., Johnston, M. and Sclafani, R.A. (1989) Galactose as a gratuitous inducer of GAL gene expression in yeasts growing on glucose. *Gene*, **83**, 57–64.
- Strand, M.K., Stuart, G., Longley, M.J., Graziewicz, M.A., Dominick, O.C. and Copeland, W.C. (2003) POS5 gene of *Saccharomyces cerevisiae* encodes a mitochondrial NADH kinase required for stability of mitochondrial DNA. *Eukaryotic Cell*, **2**, 809–820.
- Strand, M.K. and Copeland, W.C. (2002) Measuring mtDNA mutation rates in *Saccharomyces cerevisiae* using the mtArg8 assay. *Methods Mol. Biol.*, **197**, 151–157.
- Yakes, F.M. and Van Houten, B. (1997) Mitochondrial DNA damage is more extensive and persists longer than nuclear DNA damage in human cells following oxidative stress. *Proc. Natl Acad. Sci. USA*, **94**, 514–519.
- Ayala-Torres, S., Chen, Y., Svoboda, T., Rosenblatt, J. and Van Houten, B. (2000) Analysis of gene-specific DNA damage and repair using quantitative polymerase chain reaction. *Methods*, **22**, 135–147.
- Cheng, S., Chen, Y., Monforte, J.A., Higuchi, R. and Van Houten, B. (1995) Template integrity is essential for PCR amplification of 20- to 30-kb sequences from genomic DNA. *PCR Methods Appl.*, **4**, 294–298.
- Santos, J.H., Mandavilli, B.S. and Van Houten, B. (2002) Measuring oxidative mtDNA damage and repair using quantitative PCR. *Methods Mol. Biol.*, **197**, 159–176.
- Santos, J.H., Hunakova, L., Chen, Y., Bortner, C. and Van Houten, B. (2003) Cell sorting experiments link persistent mitochondrial DNA damage with loss of mitochondrial membrane potential and apoptotic cell death. *J. Biol. Chem.*, **278**, 1728–1734.
- Lewis, L.K., Kirchner, J.M. and Resnick, M.A. (1998) Requirement for end-joining and checkpoint functions, but not RAD52-mediated recombination, after EcoRI endonuclease cleavage of *Saccharomyces cerevisiae* DNA. *Mol. Cell. Biol.*, **18**, 1891–1902.

40. Foiani, M., Pelliccioli, A., Lopes, M., Lucca, C., Ferrari, M., Liberi, G., Muzi Falconi, M. and Plevani, P. (2000) DNA damage checkpoints and DNA replication controls in *Saccharomyces cerevisiae*. *Mutat. Res.*, **451**, 187–196.
41. Pook, M.A., Al-Mahdawi, S., Carroll, C.J., Cossee, M., Puccio, H., Lawrence, L., Clark, P., Lowrie, M.B., Bradley, J.L., Cooper, J.M. *et al.* (2001) Rescue of the Friedreich's ataxia knockout mouse by human YAC transgenesis. *Neurogenetics*, **3**, 185–193.
42. Storici, F., Henneke, G., Ferrari, E., Gordenin, D.A., Hubscher, U. and Resnick, M.A. (2002) The flexible loop of human FEN1 endonuclease is required for flap cleavage during DNA replication and repair. *EMBO J.*, **21**, 5930–5942.
43. Inga, A. and Resnick, M.A. (2001) p53 mutants exhibiting enhanced transcriptional activation and altered promoter selectivity are revealed using a sensitive, yeast based functional assay. *Oncogene*, **20**, 501–513.
44. Inga, A., Storici, F. and Resnick, M.A. (2003) Functional analysis of the human p53 tumor suppressor and its mutants using yeast. In Heitman, J. and Nitiss, J.L. (eds), *Yeast as a Tool in Cancer Research*. Kluwer Academic Publishers, in press.
45. Cavadini, P., Gellera, C., Patel, P.I. and Isaya, G. (2000) Human frataxin maintains mitochondrial iron homeostasis in *Saccharomyces cerevisiae*. *Hum. Mol. Genet.*, **9**, 2523–2530.
46. Schulz, J.B., Dehmer, T., Schols, L., Mende, H., Hardt, C., Vorgerd, M., Burk, K., Matson, W., Dichgans, J., Beal, M.F. *et al.* (2000) Oxidative stress in patients with Friedreich ataxia. *Neurology*, **55**, 1719–1721.
47. Emond, M., Lepage, G., Vanasse, M. and Pandolfo, M. (2000) Increased levels of plasma malondialdehyde in Friedreich ataxia. *Neurology*, **55**, 1752–1753.
48. Tozzi, G., Nuccetelli, M., Lo Bello, M., Bernardini, S., Bellincampi, L., Ballerini, S., Gaeta, L.M., Casali, C., Pastore, A., Federici, G. *et al.* (2002) Antioxidant enzymes in blood of patients with Friedreich's ataxia. *Arch. Dis. Child.*, **86**, 376–379.
49. Piemonte, F., Pastore, A., Tozzi, G., Tagliacozzi, D., Santorelli, F.M., Carozzo, R., Casali, C., Damiano, M., Federici, G. and Bertini, E. (2001) Glutathione in blood of patients with Friedreich's ataxia. *Eur. J. Clin. Invest.*, **31**, 1007–1011.
50. Pinz, K.G., Shibutani, S. and Bogenhagen, D.F. (1995) Action of mitochondrial DNA polymerase gamma at sites of base loss or oxidative damage. *J. Biol. Chem.*, **270**, 9202–9206.
51. Boudsocq, F., Ling, H., Yang, W. and Woodgate, R. (2002) Structure-based interpretation of missense mutations in Y-family DNA polymerases and their implications for polymerase function and lesion bypass. *DNA Repair (Amst.)*, **1**, 343–358.
52. Penta, J.S., Johnson, F.M., Wachsman, J.T. and Copeland, W.C. (2001) Mitochondrial DNA in human malignancy. *Mutat. Res.*, **488**, 119–133.
53. Bradley, J.L., Blake, J.C., Chamberlain, S., Thomas, P.K., Cooper, J.M. and Schapira, A.H. (2000) Clinical, biochemical and molecular genetic correlations in Friedreich's ataxia. *Hum. Mol. Genet.*, **9**, 275–282.
54. Santos, M.M., Ohshima, K. and Pandolfo, M. (2001) Frataxin deficiency enhances apoptosis in cells differentiating into neuroectoderm. *Hum. Mol. Genet.*, **10**, 1935–1944.
55. Rosen, D.R. (1993) Mutations in Cu/Zn superoxide dismutase gene are associated with familial amyotrophic lateral sclerosis. *Nature*, **364**, 362.
56. Mecocci, P., MacGarvey, U. and Beal, M.F. (1994) Oxidative damage to mitochondrial DNA is increased in Alzheimer's disease. *Ann. Neurol.*, **36**, 747–751.
57. Sheehan, J.P., Swerdlow, R.H., Miller, S.W., Davis, R.E., Parks, J.K., Parker, W.D. and Tuttle, J.B. (1997) Calcium homeostasis and reactive oxygen species production in cells transformed by mitochondria from individuals with sporadic Alzheimer's disease. *J. Neurosci.*, **17**, 4612–4622.
58. Sheehan, J.P., Swerdlow, R.H., Parker, W.D., Miller, S.W., Davis, R.E. and Tuttle, J.B. (1997) Altered calcium homeostasis in cells transformed by mitochondria from individuals with Parkinson's disease. *J. Neurochem.*, **68**, 1221–1233.
59. Beal, M.F. (1992) Does impairment of energy metabolism result in excitotoxic neuronal death in neurodegenerative illnesses? *Ann. Neurol.*, **31**, 119–130.
60. Sherman, F., Fink, G.F., Hicks, J.B. (1986) *Methods in Yeast Genetics*. Cold Spring Harbor Laboratory, Cold Spring Harbor, NY.
61. Gietz, R.D. and Schiestl, R.H. (1991) Applications of high efficiency lithium acetate transformation of intact yeast cells using single-stranded nucleic acids as carrier. *Yeast*, **7**, 253–263.
62. Gary, R., Park, M.S., Nolan, J.P., Cornelius, H.L., Kozyreva, O.G., Tran, H.T., Lobachev, K.S., Resnick, M.A. and Gordenin, D.A. (1999) A novel role in DNA metabolism for the binding of Fen1/Rad27 to PCNA and implications for genetic risk. *Mol. Cell. Biol.*, **19**, 5373–5382.
63. Daum, G., Bohni, P.C. and Schatz, G. (1982) Import of proteins into mitochondria. Cytochrome b2 and cytochrome c peroxidase are located in the intermembrane space of yeast mitochondria. *J. Biol. Chem.*, **257**, 13028–13033.
64. Branda, S.S., Yang, Z.Y., Chew, A. and Isaya, G. (1999) Mitochondrial intermediate peptidase and the yeast frataxin homolog together maintain mitochondrial iron homeostasis in *Saccharomyces cerevisiae*. *Hum. Mol. Genet.*, **8**, 1099–1110.
65. Nixon, D.E., Moyer, T.P., Johnson, P., McCall, J.T., Ness, A.B., Fjerstad, W.H. and Wehde, M.B. (1986) Routine measurement of calcium, magnesium, copper, zinc, and iron in urine and serum by inductively coupled plasma emission spectroscopy. *Clin. Chem.*, **32**, 1660–1665.
66. Bogenhagen, D. and Clayton, D.A. (1974) The number of mitochondrial deoxyribonucleic acid genomes in mouse L and human HeLa cells. Quantitative isolation of mitochondrial deoxyribonucleic acid. *J. Biol. Chem.*, **249**, 7991–7995.
67. Graziewicz, M.A., Day, B.J. and Copeland, W.C. (2002) The mitochondrial DNA polymerase as a target of oxidative damage. *Nucl. Acids. Res.*, **30**, 2817–2824.